

Clustering Analysis of Periodic Point Vortices with the L Function

MAKOTO UMEKI*

*Department of Physics, Graduate School of Science, University of Tokyo,
7-3-1 Hongo, Bunkyo-ku, Tokyo 113-0033, Japan*

The motion of point vortices with periodic boundary conditions was studied by using Weierstrass zeta functions. The scattering and recoupling of a vortex pair by a third vortex becomes remarkable when the vortex density is large. The clustering of vortices with various initial conditions is quantitated by the L function used in the point process theory in spatial ecology. It is shown that clustering persists if the initial distribution is clustered like an infinite row or a checkered pattern.

KEYWORDS: point vortex, two-dimensional turbulence, L function, point process theory

The statistical approach to the problem of assemblies of point vortices (PVs) dates back to Onsager (1949). A state of negative temperature is considered to be related to the clustering of vortices rotating in the same direction and the inverse energy cascade predicted in the two-dimensional Navier-Stokes (2D NS) turbulence. In many numerical simulations, PVs are bounded in a circular wall since a velocity field due to a PV can be computed by including a single mirror image. Although the axisymmetry with respect to the origin is conserved, spatial homogeneity is not guaranteed in such a circular system. The numerical difficulty in the simulation of vortices in a box is that there emerges an infinite sequence of virtual images. Our objective is to study the turbulent motions and clustering of many PVs in a periodic box using Weierstrass zeta functions.

Let us start by representing the 2D NS equation in terms of a complex position $z = x + iy$, velocity $q = u - iv$, pressure p , and kinematic viscosity ν as

$$q_t + qq_{\bar{z}} + \bar{q}q_z = -2p_z + 4\nu q_{z\bar{z}}. \quad (1)$$

Here, \bar{q} denotes the complex conjugate of q and we use the relations $\partial_x = \partial_z + \partial_{\bar{z}}$, $\partial_y = i(\partial_z - \partial_{\bar{z}})$, $u = (q + \bar{q})/2$, $v = i(q - \bar{q})/2$, and $\Delta = 4\partial_{z\bar{z}}$. The incompressible condition yields $\nabla \cdot \mathbf{v} = \bar{q}_z + q_{\bar{z}} = 0$. The vorticity $\omega = v_x - u_y$ can be expressed by q as $\omega = 2iq_{\bar{z}}$.

If the flow is irrotational $\omega = 0$, then $q_{\bar{z}} = 0$, q depends on only z (and t), and the theory of conformal mapping can be applied. Equations for the vorticity and pressure are

$$q_{z\bar{t}} + qq_{\bar{z}\bar{z}} + \bar{q}q_{z\bar{z}} = 4\nu q_{z\bar{z}\bar{z}}, \quad (2)$$

and $p_{z\bar{z}} = -(q_z\bar{q}_{\bar{z}} + \bar{q}_{\bar{z}}^2)/2$, respectively.

According to Tkachenko,^{1,2} the velocity field due to a single PV at the origin with periodic boundary conditions (BCs) is equivalent to that due to the PVs on the lattice $z_{mn} = 2m\omega_1 + 2n\omega_2$, where the complex numbers ω_1, ω_2 are the half periods of the lattice and m, n are arbitrary integers. The ratio of the two periods $\tau = \omega_1/\omega_2$ can be restricted in the region

$$\text{Im}\tau > 0, \quad |\text{Re}\tau| < 1/2, \quad |\tau| \geq 1. \quad (3)$$

We investigate the case of square periodic BCs, which are usually employed in the numerical studies of two-dimensional turbulence by selecting $\tau = i$. However, we can deal with an arbitrary periodic parallelogram by considering various values of τ that satisfy (3).

The velocity field due to a PV of strength $\kappa = 2\pi$ is given by the Weierstrass zeta function $\zeta(z; \omega_1, \omega_2)$ along with a rigid rotation term as follows:

$$\bar{q} = i\overline{\zeta(z)} - i\Omega z \equiv w(z). \quad (4)$$

Since the vortex lattice undergoes rigid rotation with an angular velocity $\Omega = \pi/[4\text{Im}(\bar{\omega}_1\omega_2)]$, the second term in Eq. (4) is necessary in order to cancel the velocity circulation on the boundary. The vortex density $n = 1/[4\text{Im}(\bar{\omega}_1\omega_2)]$, Ω , and the vortex strength κ are related as $\kappa n = 2\Omega$. If the length of the side of the square is unity, then $\omega_1 = 1/2$, $\omega_2 = i/2$, $\Omega = \pi$, and $\kappa = 2\pi$.

The equation for the streamline $\psi = \text{const.}$, where ψ is the streamfunction, is equivalent to $dx/\psi_y = -dy/\psi_x$. Using the relations $u = \psi_y$ and $v = -\psi_x$, ψ is expressed as $\psi = \int u dy + f(x)$. The sigma and zeta functions of Weierstrass are related as $\zeta(z) = \sigma'(z)/\sigma(z)$. This relation is consistent with the asymptotic forms $\zeta \sim 1/z$ and $\sigma \sim z$ when $z \sim 0$. Using the above results, ψ for a single vortex lattice centered at the origin is given by

$$\psi = -\text{Re} \ln \sigma(z) + \Omega|z|^2/2. \quad (5)$$

There is a minimum value of ψ in the periodic case, in contrast with the unbounded plane in which there are no limits on ψ .

For simplicity, we consider an assembly of PVs with $\kappa_i = 2\pi\mu_i$, $\mu_i = 1$, for $i = 1, \dots, N_1$ and $\mu_i = -1$ for $i = N_1 + 1, \dots, N (= N_1 + N_2)$. Therefore, ψ for N PVs located at z_i is given by

$$\psi = \sum_{i=1}^N \mu_i \{-\text{Re}[\ln \sigma(z - z_i)] + \Omega|z - z_i|^2/2\}. \quad (6)$$

Using Eq. (4), the equation of motion of PVs with square periodic BCs can be expressed as³

$$\dot{z}_i = \sum_{j \neq i} \mu_j w(z_i - z_j). \quad (7)$$

The equation can be rewritten in the Hamiltonian form as $\mu_i dz_i/dt = \partial H/\partial \bar{z}_i$, where the Hamiltonian H can be expressed as $H = \sum_{i=1}^N \mu_i h_i = \sum_{i=1}^N \sum_{j=i+1}^N \mu_i \mu_j h_{ij}$,

*E-mail address: umeki@phys.s.u-tokyo.ac.jp

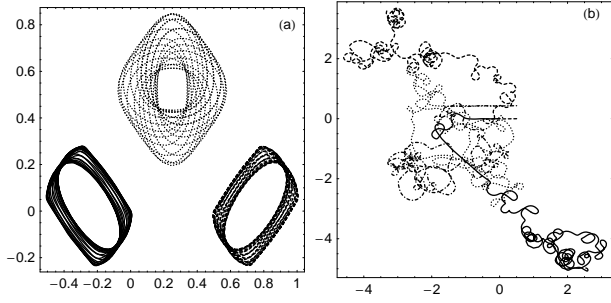


Fig. 1. Trajectories of three (a) and four PVs (b). PVs 1, 2, 3, and 4 are denoted by solid, dashed, dotted, and dotted-dashed curves, respectively.

$h_{ij} = -\text{Re}[\ln \sigma(z_i - z_j)] + \Omega|z_i - z_j|^2/2$. The Hamiltonian, which is given by the total kinetic energy minus the self-induced kinetic energy of PVs, can be interpreted as the sum of a kinetic energy due to interactions between the pairs of PVs.

If *Mathematica* is used, we can compute the Weierstrass zeta function as we use the sinusoidal function in a Fortran code. The system (4,7) is solved numerically by the *NDSolve* command of *Mathematica* 5.2 installed in a PC with an AMD Athlon 64x2 3800 CPU, 2 GB memory and Windows XP OS. The computation is realistic since the CPU time in such a PC environment ranges from two to five days for 100 PVs and 10 eddy turnover times.

If the PVs lie in an unbounded domain, the system has four integrals:⁴ the Hamiltonian $H_u = -\sum \mu_i \mu_j \ln |z_i - z_j|$, two components of the linear impulse $\mathbf{I} = (I_x, I_y)$, $I_x = \sum \mu_i \text{Re}[z_i]$, $I_y = \sum \mu_i \text{Im}[z_i]$, and the angular impulse $A = \sum \mu_i |z_i|^2$. Since the system in a periodic box has no circular symmetry, A is no more constant; however, H , I_x , and I_y are conserved. Since there are three conserved quantities, the system of three PVs is integrable, while the four PVs exhibit chaos.

Examples of the trajectories of three PVs with $\mu_i = (2, 2, -1)$ and an initial condition $(z_1, z_2, z_3) = (0, 0.5, 0.25 + i\sqrt{3}/4)$ located at the vertices of an equilateral triangle and that of four PVs with $\mu_i = (2, 2, -1, -1)$ and $(z_1, z_2, z_3, z_4) = (0, 0.5, i\sqrt{3}/4, 0.5 + i\sqrt{3}/4)$ at $t = 0$ located at the vertices of a rectangle are shown in Figures 1a and 1b, respectively. The first case leads to a collapse if the PVs are in an unbounded plane.

To analyze the spatial distribution of many PVs, we introduce the L function used in the point process theory in spatial ecology.^{5,6} Let $\vec{x}_i = (x_i, y_i)$ be the position of N points randomly distributed in an area S . The K function is defined by

$$K(r) = (\lambda N)^{-1} \sum_{i=1}^N \sum_{j=1, j \neq i}^N \theta(r - |\vec{x}_i - \vec{x}_j|), \quad (8)$$

where $\lambda = N/S$ is the number density of the points and $\theta(x)$ is the step function. An extra function added in (8), in order to modify the edge effect, is unnecessary in the present periodic case.

If the distribution of points obeys completely spatially randomness (CSR), which is synonymous with a homogeneous Poisson process, $K(r)$ becomes the area of the circle with radius r , i.e., $K(r) = \pi r^2$. Then, it is conve-

nient to introduce the L function as

$$L(r) = \sqrt{K(r)/\pi} - r. \quad (9)$$

CSR yields $L = 0$. For clustering, i.e. points staying close to the other points, we have $L > 0$. If the points tend to be at a distance from each other, $L < 0$. Whether $L(r)$ is positive or negative can depend on r . For instance, a checkered pattern (*Ichimatsu moyo* in Japanese) gives $L > 0$ for small r , but $L < 0$ for large r .

According to Novikov (1976),⁷ for an unbounded plane, we have a relation between the distance r_{jl} of two PVs of strength κ_j and κ_l and the energy spectrum $E(k)$ as

$$E(k) = (4\pi k)^{-1} [\sum_j \kappa_j^2 + 2\sum_{j < l} \kappa_j \kappa_l J_0(kr_{jl})]. \quad (10)$$

If $\kappa_j = \kappa$ for all j , we have

$$E(k) = \kappa^2 (4\pi k)^{-1} [N + 2\sum_{j < l} J_0(kr_{jl})]. \quad (11)$$

Using the number density $\rho(r)$ at the distance r between two PVs, we have, in the continuous limit, $E(k) = E_1(k) + E_2(k)$, where $E_1(k) = \kappa^2 N (4\pi k)^{-1}$ and $E_2(k) = \kappa^2 (2\pi k)^{-1} \int_0^\infty J_0(kr) \rho(r) dr$. $E_1(k)$ and $E_2(k)$ correspond to the self-energy of each vortex and the interaction energy between two PVs, similar to h_{ij} . The relation between the $K(r)$ and $\rho(r)$ is $K(r) = l^2 N'^{-1} \int_0^r \rho(r') dr'$, where $\rho(r)$ is normalized by the upper limit l of r and the total number $N' = N(N-1)/2$ of pairs of PVs.

If $\rho(r) = Cr^\alpha$, we can integrate $E_2(k)$ into $E_2(k) = \kappa^2 C k^{-\alpha-2} \Gamma((\alpha+1)/2) [2\pi \Gamma((1-\alpha)/2)]^{-1}$ for $-1 < \alpha < 1/2$. The value $\alpha = -1/3$ gives the Kolmogorov spectrum $k^{-5/3}$ in a 3D turbulence.

Formally, the CSR value $\alpha = 1$ in two dimensions yields the k^{-3} spectrum, although the integral does not converge. In order to avoid divergence, an exponential decay in $\rho(r)$ may be introduced. Otherwise, we may set the upper limit l in the range of integration in $E_2(k)$. Using the normalization $r = lr'$ and the integral expressed by a regularized hypergeometric function as $\int_0^1 J_0(kr) r^\alpha dr = \Gamma((1+\alpha)/2) {}_1F_2((1+\alpha)/2; \{1, (3+\alpha)/2\}; -k^2/4) [2\Gamma((3+\alpha)/2)]^{-1}$, for $\alpha > -1$, $E_2(k)$ is written as $E_2(k) = \kappa^2 C l^{\alpha+1} \Gamma((1+\alpha)/2) {}_1F_2((1+\alpha)/2; \{1, (3+\alpha)/2\}; -(kl)^2/4) [4\pi k \Gamma((3+\alpha)/2)]^{-1}$.

If we use the CSR distribution $\rho(r) = \pi N' l^{-2} r$, we have $\int_0^1 J_0(kr) r dr = J_1(k)/k$. Then, $E_2(k)$ is given by

$$E_2(k) = \kappa^2 N' l^{-1} k^{-2} J_1(kl)/2. \quad (12)$$

For large kl , we have the asymptotic form

$$E_2(k) \simeq \sqrt{1/2\pi} \kappa^2 N' l (kl)^{-5/2} \cos(kl - 3\pi/4). \quad (13)$$

The value of $E_2(k)$ is oscillatory as k increases with the amplitude decaying as $k^{-5/2}$. Evidently, the total energy spectrum does not become negative because $E_1(k) \gg E_2(k)$ for large k .

For numerical studies, we first consider an assembly of PVs having the same positive strength $\kappa (= 2\pi)$. The following four typical cases are considered: Case (I) an infinite row that is a discrete model of the vortex sheet, Case (II) PVs located randomly in checkered patterns, Case (III) PVs located randomly in the 10×10 sub-

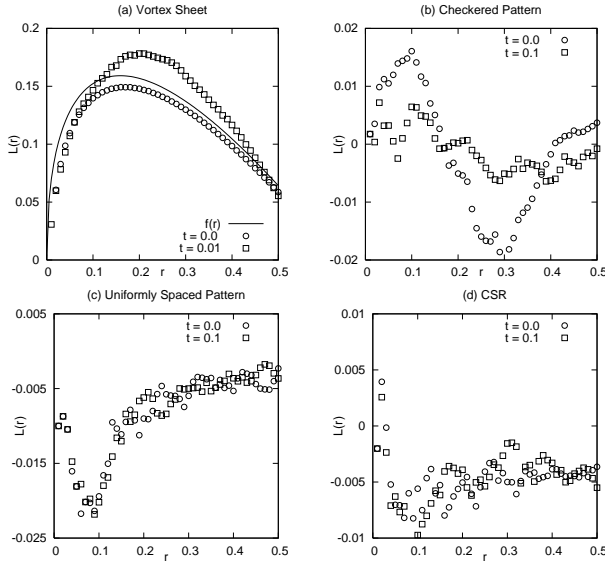


Fig. 2. The L functions. (a) corresponds to (I), (b) to (II), (c) to (III), and (d) to (IV)

squares, and Case (IV) CSR in the unit square. Here, the word *CSR* implies that the PVs are distributed by using random numbers generated by a single run. The initial conditions, the number N of PVs, the final time t_f , and the values of three conserved quantities are summarized in Table 1. The relative precision of H in the numerical simulation is confirmed to be less than $10^{-6} \sim 10^{-5}$ up to $t = t_f$. Figure 2 shows the L function computed by the initial and final distributions of PVs.

For Case (I), the PVs are initially located on the x -axis as $z_j(0) = j/N + \epsilon \sin 2\pi j/N$, $j = 1, \dots, N$, where $\epsilon = 0.05$. If ϵ is fixed and N is increased, the pairing of two adjacent PVs becomes more conspicuous than the winding of the sheet due to the Kelvin-Helmholtz instability. The growth rate $\sigma = \kappa\pi p(1-p)/a^2$ of the pairing instability in an unbounded plane attains a maximum at the wavenumber $p = 1/2$, where a is the distance between two adjacent PVs.⁴ Modulus 1 is suitably considered so that the PVs are plotted in the selected square. Of course, the PVs wander chaotically from one square to another.

For $\epsilon = 0$, we have $\rho(r) = 2N'l^{-2}$, $K(r) = 2r$ and the average Hamiltonian $\langle h \rangle = 2 \sum_{i>j} h_{ij} [N(N-1)]^{-1} = 2 [\sum_{j=1}^{N/2-1} \psi(j/N) + \psi(1/2)/2] [N(N-1)]^{-1} \sim 2 \int_0^{1/2} dx \psi(x)$. Since $\psi(x) \sim -\ln|x|$ for $x \sim 0$, $\langle h \rangle \equiv \int_S dx dy \psi(x, y) \rho(r)$ yields a finite value for $\rho = Cr^\alpha$, $r \sim 0$, and $\alpha > -2$. Since $\alpha < 1$ corresponds to clustering, clustering with $\alpha < -2$ cannot occur from the initial condition with a finite $\langle h \rangle$.

Second, we consider Case (II) where the initial PVs are located randomly in eight segments revealing a checkered pattern. $L(r) > 0$ for $0 < r < 0.15$ implies that the PVs are clustered, while $L(r) < 0$ for $0.15 < r < 0.4$ means that they are uniformly spaced at larger scales. We observe that this tendency remains at $t = t_f$, although it becomes somewhat weak and an additional oscillatory behavior is observed.

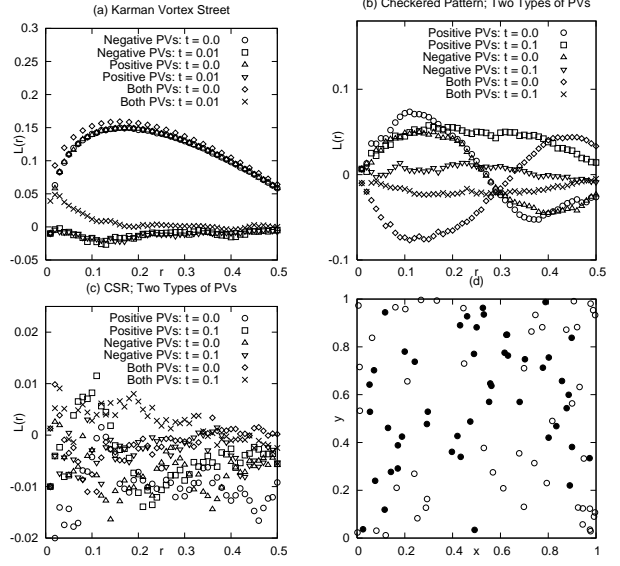


Fig. 3. The L functions. (a) corresponds to (V), (b) to (VI), and (c) to (VII). (d) shows the distribution of PVs for (VI) at $t = 0.1$. White (black) circles denote positive (negative) PVs.

Third, Case (III) initially has uniformly spaced PVs. $L(r)$ has a negative value and a minimum at $r \approx 0.06$. We observe that $L(r)$ is almost the same during $t \in [0, t_f]$.

Fourth, we examine the completely spatially random distribution of the PVs at $t = 0$ in Case (IV). We observe slightly negative values of $L(r)$ at $t = 0$ and t_f , but we do not see any significant differences between the initial and final distributions.

Next, we consider the system with both positive and negative PVs of the same strength and the same numbers $N_1 = N_2 = N/2$. The following three typical cases are examined: Case (V) the Kármán vortex street, Case (VI) positive and negative PVs located alternately in checkered segments (16 subsquares), and Case (VII) completely spatially random distribution. The initial conditions, the number of PVs, t_f , and the values of three conserved quantities are summarized in Table 2.

First, we consider Case (V) given by the following expression: $(\mu_j, z_j(0)) = (-1, j/N_1 + \epsilon(R + iR))$ for $j = 1, \dots, N_1$ and $(\mu_j, z_j(0)) = (1, j/N_2 + 1/N + ih + \epsilon(R + iR))$ for $j = N_1 + 1, \dots, N$, where $\epsilon = 10^{-4}$, R denotes random numbers, and the distance h between two rows is taken as $1/N$. In this case, the negative PVs are first numbered. At approximately $t = 0.001$, we observe that the two rows begin to break with the pairing instability.⁴

For the two types of PVs, we introduce $K_{lm}(r)$ for $(l, m) = (+, +), (-, -),$ and $(+, -)$ as

$$K_{lm}(r) = (\lambda N_1)^{-1} \sum_i \sum_j \theta(r - |\vec{x}_i - \vec{x}_j|), \quad (14)$$

where the sum is for $i, j = 1, \dots, N_1$ except for $j = i$ if $(l, m) = (+, +)$. The case $(l, m) = (-, -)$ is similar. The sum for $(l, m) = (+, -)$ is both for $i = 1, \dots, N_1$, $j = N_1 + 1, \dots, N$ and $i = N_1 + 1, \dots, N$, $j = 1, \dots, N_1$. We define $L_{lm}(r)$ from $K_{lm}(r)$ similar to Eq. (9). We observe strong clustering for $(l, m) = (+, -)$ at $t = 0.01$ corresponding to the pairing instability.

Second, for Case (VI), we observe the asymmetry, i.e., $L_{++}(r) \gg L_{--}(r)$ for all r at $t = 0.1$. The initial clustering is incidentally stronger for positive PVs than the negative ones. This fact can be regarded as clustering to a single vortex at the largest scale. There is also a significant void where positive (or negative) PVs do not exist at $t = t_f$. We can also consider the initial *fractal* distribution like a Sierpinski's gasket, which shows clustering at large scales.

Finally, we consider the CSR distributions of two types of PVs as that in Case (VII). A remarkable feature in this turbulent situation is that there are several pairs of positive and negative vortices moving linearly at a velocity of $\kappa/4h\pi$, where $2h$ is the distance between two PVs. Since the pair is surrounded by a number of other isolated PVs, however, the moving direction is bent by a third vortex when they cross each other. Moreover, if the collision is nearly head-on, a vortex of the pair with a sign opposite to the third target vortex replaces its partner with the latter and then continues to move linearly again. An exact analysis of such scattering of three PVs in an unbounded domain was already given by Aref (1979).⁸

The examples of scattering and recoupling of three PVs in a periodic box are given by an initial location $(z_1, z_2, z_3) = (L + iL, (L + d + h)i, (L + d - h)i)$ with $L = 1/2$. A pair of vortices 2 and 3 is initially approaching vortex 1. Figure 4a shows their trajectories when $h = 0.02$ and $d = \pm 0.02, \pm 0.01, 0.04, 0.08, 0.16$, and 0.32 . The final time t_f is 0.04 except for $t_f = 0.1$ for $d = 0.16$, $t_f = 0.05$ for $d = 0.32$, and $t_f = 0.06$ for $d = -0.01$. Recoupling is observed for $d = 0.01, 0.02, 0.04, 0.08$, and 0.16 . The dependence of a π -normalized scattering angle $\delta\phi/\pi$ measured by the moving direction of $z_3(t = 0.04)$ for $h = 0.02$ in a periodic box is shown in Figure 4b. The recoupling of PVs in an unbounded plane with $L \rightarrow \infty$ ⁸ occurs if $0 < d/h < 9$. On the other hand, the present simulation in a periodic box with $h = 0.02$ shows a shift of the range d for recoupling as $-0.5 \lesssim d/h \lesssim 8.5$, although this range may vary as h is changed in the case of periodic BCs. In a GIF animation, successive scattering and recoupling, similar to the chaos in a billiard system, are clearly observed. The existence of such vortex pairs may play a crucial role in stirring assemblies of PVs.

Since the average distance of randomly located PVs is $l \sim N^{-1/2}$ and the strength 2π is fixed, the typical velocity and eddy turnover time are $v \sim N^{1/2}$ and $t_e \sim 1/N$, respectively. Denoting the smallest distance of the vortex pair by αl , its velocity is $V \sim 1/\alpha l$. Because of the recoupling condition, the cross section of the scattering is approximately $\sigma_c \sim d \sim 10\alpha l$ and the area swept by the pair during t_e is $S \sim dVt_e \sim 10/N$. Therefore, the condition for the scattering to occur in t_e is $N \sim 10$ since $S \sim 1$, the size of the square. If $N = 100$, $t_e \sim 0.01$ and one pair will be scattered approximately 10 times in a numerical simulation in the time interval $0 \leq t \leq 0.1 \sim 10t_e$.

The $L_{lm}(r)$ function becomes slightly positive for $(l, m) = (+, -)$, which also indicates that the pairs of positive and negative PVs survive until $t = 0.1$. How-

ever, the absolute values are much smaller than the initially clustered cases. To clearly observe the spontaneous

Table I. Single type of PVs

Case	N	t_f	H	I_x	I_y
I	100	0.01	17948	50.5	0
II	96	0.1	11973	47.872	47.923
III	100	0.1	12796	49.968	50.020
IV	100	0.1	12886	49.687	50.206

Table II. Two types of PVs

Case	$N_{1,2}$	t_f	H	I_x	I_y
V	50	0.01	-415.31	-0.50019	-0.49976
VI	48	0.1	369.60	-12.176	-11.081
VII	50	0.1	-178.31	-1.9433	2.3455

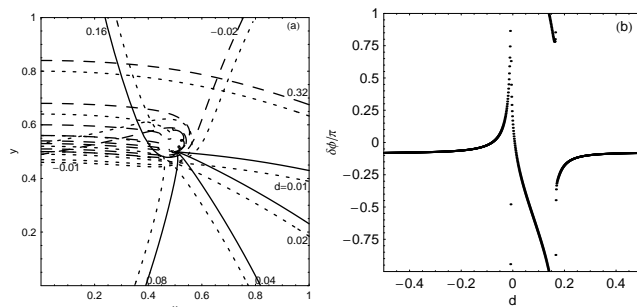


Fig. 4. (a) Trajectories of three scattering and recoupling PVs for various values of h . Solid, dashed, and dotted curves denote z_1 , z_2 , and z_3 , respectively. (b) The π -normalized scattering angle $\delta\phi/\pi$ versus d for $h = 0.02$.

clustering, longer simulations may be required. We also investigated the probability distribution function of velocity circulation, which is studied in Umeki (1993)⁹ for a 3D turbulence.¹⁰ A similar approach in the point process theory is called the Quadrat method.⁵

In summary, a method to simulate the motions of PVs with periodic BCs is described. Several numerical examples are illustrated and the clustering of PVs with different conditions is examined by the L function.

The author is grateful to Professor Yamagata for support through his research on fluid dynamics over several years.

- 1) V. K. Tkachenko: *Sov. Phys. JETP* **22** (1966) 1282.
- 2) V. K. Tkachenko: *Sov. Phys. JETP* **23** (1966) 1049.
- 3) M. A. Stremler and H. Aref: *J. Fluid Mech.* **392** (1999) 101.
- 4) P. G. Saffman: *Vortex Dynamics* (Cambridge University Press, Cambridge, 1992) Chap. 7.
- 5) N. A. C. Cressie: *Statistics for Spatial Data, Revised Edition* (Wiley, New York, 1993).
- 6) K. Shimatani: *Jpn. J. Ecology* **51** (2001) 87 [in Japanese].
- 7) E. A. Novikov: *Sov. Phys. JETP* **41** (1976) 937.
- 8) H. Aref: *Phys. Fluids* **22** (1979) 393.
- 9) M. Umeki: *J. Phys. Soc. Jpn.* **62** (1993) 3788.
- 10) A. A. Migdal: *Int. J. Mod. Phys. A* **10** (1994) 1197.